fishes

MDPI

Communication

Maternal Loading Heterogeneity and Early Developmental Expression Profiles of Hepcidin Transcripts in Siberian Sturgeon (*Acipenser baerii*)

Eun Jeong Kim [1] and Yoon Kwon Nam [2,*]

[1] Institute of Marine and Aquatic LMO, Pukyong National University, Busan 48513, Republic of Korea; kejeong@pukyong.ac.kr
[2] Faculty of Fisheries Life Sciences, Pukyong National University, Busan 48513, Republic of Korea
* Correspondence: yoonknam@pknu.ac.kr

Abstract

Hepcidin is a multifunctional peptide involved in innate immunity and iron homeostasis, yet its earliest developmental regulation in sturgeons remains poorly understood. Here, we investigated maternal loading and embryonic expression patterns of hepcidin transcripts (*hamp*) in Siberian sturgeon (*Acipenser baerii*). RT-qPCR detected *hamp* transcripts in all 17 unfertilized egg (UFE) batches examined; however, maternally loaded transcript abundance varied markedly among batches, with up to a 14.8-fold difference, indicating substantial heterogeneity in the molecular starting state of embryos. In contrast, female traits, including age, body weight, and condition factor, as well as fertilization rate and hatching success, were not significantly correlated with UFE *hamp* transcript abundance (Spearman's rank correlation with BH-FDR adjustment; $q > 0.05$). Developmental expression analysis from UFE to first hatch was then performed using five developmental series (DevSeries 1–5) that represented relatively high, intermediate, and low UFE baseline levels within the statistically differentiated UFE dataset (Welch ANOVA/Games–Howell post hoc, $p < 0.05$). The developmental dataset showed significant DevSeries, stage, and DevSeries × stage effects, indicating that embryonic *hamp* expression profiles differed among DevSeries (two-way ANOVA, $p < 0.05$). High-loading DevSeries (DevSeries 2 and 4) showed prolonged early persistence followed by later re-elevation, whereas low-loading DevSeries (DevSeries 3 and 5) maintained lower overall abundance but displayed more evident stage-linked increases during embryogenesis. Collectively, these findings show that maternally loaded *hamp* transcripts are associated with embryonic expression profiles and support the view that maternal transcript abundance provides an initial baseline that should be considered when interpreting early developmental expression profiles of immune- and iron-regulation-related genes in this chondrostean species.

Keywords: *Acipenser baerii*; development; hepcidin; maternal loading; unfertilized eggs

Key Contribution: This study shows that maternally loaded *hamp* transcripts, encoding hepcidin, vary markedly among Siberian sturgeon unfertilized egg batches and are associated with distinct early developmental expression profiles. These findings highlight maternal transcript-provisioning heterogeneity as an important baseline for interpreting hepcidin expression during early sturgeon development.

Academic Editor: Huapu Chen

Received: 2 May 2026
Revised: 24 June 2026
Accepted: 26 June 2026
Published: 3 July 2026

1. Introduction

Hepcidin is a conserved vertebrate peptide with dual roles in innate immunity and iron homeostasis. In addition to its antimicrobial activity, hepcidin regulates systemic iron availability through its interaction with ferroportin, thereby influencing iron absorption, mobilization, and tissue distribution [1,2]. Given the fundamental importance of iron balance in cellular metabolism and developmental progression, hepcidin may also have important roles during early vertebrate development, although direct evidence for embryonic function in fishes remains limited [3–6].

In externally developing fish embryos, early development depends heavily on maternally supplied transcripts and other egg-borne factors before embryonic regulatory activity becomes predominant [7–10]. Within this context, maternal provisioning of hepcidin-related transcripts may be relevant to early developmental regulation because both innate immunity and iron regulation are expected to undergo biologically important transitions during the developmental progression from maternally provisioned embryos to hatched larvae [11–13]. However, the earliest developmental deployment of hepcidin, including the influence of maternal loading abundance on subsequent embryonic expression, remains poorly understood, particularly outside a few teleost models [14–16].

Sturgeons occupy a basal position within the actinopterygian lineage and are known to exhibit a slow rate of molecular evolution. In this evolutionary context, this early-diverging fish group may retain information closer to ancestral or prototypic states of genes that have undergone lineage-specific sub- and/or neofunctionalization, often accompanied by paralog diversification in teleost groups [17–19]. For this reason, sturgeons may serve as a useful comparative model for building an early evolutionary repertoire of the potential link between hepcidin and reproductive/developmental physiology in the actinopterygian clade. However, despite its importance, little is known about maternal loading and embryonic expression of *hamp* transcripts in sturgeon species. Our previous study identified a conserved *hamp* ortholog from Siberian sturgeon (*Acipenser baerii*), a commercially important aquacultured sturgeon species in South Korea, and demonstrated its basal expression in immature gonads and inducible expression during immune challenge and iron overload in several juvenile and subadult tissues [20,21]. However, its maternal supply to eggs and developmental expression characteristics have remained unresolved.

Based on this need, the objectives of this study were: (1) to determine whether *hamp* transcripts are consistently maternally loaded in farmed Siberian sturgeon; (2) to investigate whether the abundance of maternally supplied *hamp* transcripts differs markedly among egg batches from different female broodfish; and (3) to examine whether differences in maternal *hamp* transcript loading are potentially associated with subsequent developmental expression patterns during embryogenesis. To address these objectives, we first quantified *hamp* transcript abundance in 17 unfertilized egg batches from 15 female broodfish with different age and body-weight classes, and then examined developmental expression profiles in five independent full-sib crosses with contrasting initial *hamp* loading levels in unfertilized eggs.

2. Materials and Methods

2.1. Experimental Unfertilized Egg and Developing Embryo Samples

Siberian sturgeon (*Acipenser baerii*) gametes used in this study were obtained from Dinoville Aquafarm (Hamyang, Gyeongnam, Republic of Korea), where artificial breeding was performed following hormone-induced spawning procedures as previously described [20]. In total, 17 unfertilized egg batches (UFE 01–17) were obtained from 15 different females between 2011 and 2025. Except for two 2013 UFE batches (UFE 02 and UFE 03), for which two replicate samples were available, unfertilized eggs were sampled in triplicate

for each UFE batch. Consequently, a total of 49 replicate UFE samples from the 17 batches were used to measure *hamp* transcript abundance by RT-qPCR.

Among these 17 UFE batches, 14 batches, excluding UFE 03, UFE 12, and UFE 14, were subjected to artificial fertilization [20] using sperm from 13 individual male broodfish for seedling production between 2011 and 2025. Based on the completeness of developmental-stage coverage and the representation of contrasting *hamp* abundance levels in unfertilized eggs, staged embryo samples from five crosses were further subjected to comparative analysis of maternal *hamp* loading levels and subsequent embryonic expression patterns. These five developmental crosses were labeled DevSeries 1–5, respectively: DevSeries 1 (2016, UFE batch 05), DevSeries 2 (2016, UFE 06), DevSeries 3 (2019, UFE 09), DevSeries 4 (2023, UFE 13), and DevSeries 5 (2025, UFE 17). Metadata for the broodfish, 17 UFE batches, and five DevSeries are provided in Supplementary Table S1.

Embryos from the five DevSeries were managed under almost identical controlled incubation conditions at the same facility, although they were generated in different years. After fertilization, embryos were incubated in 1 μm filtered groundwater under controlled conditions at 18–19 °C, with a 14 h:10 h light photoperiod and dissolved oxygen levels of 7.5–8.5 mg/L. Embryonic samples were collected at predefined developmental stages spanning from just fertilization to first hatch, with the corresponding UFE samples included as the maternal baseline. The selected stages were unfertilized eggs (UFE), just fertilized eggs (JF), early cleavage (EC; 2–4 cells), late cleavage (LC; 16–64 cells), early blastula (EB), onset of gastrulation (OG), small yolk plug formed (SYP; close to the end of gastrulation), onset of neurulation (ON), excretory rudiments elongate (ExcR; pronephric rudiments), heart rudiment (HR), S-shaped heart formed (SH; onset of heart beating and blood circulation), tail end reaches head (TRH), and first hatch (FH). Developmental stages were confirmed by microscopic examination according to external morphological criteria established in our previous study [20]. At each sampling point, developing embryos were collected from each DevSeries in three biological replicates, with 10–12 embryos per replicate. Collected unfertilized eggs and embryos were immediately frozen on dry ice and stored at −85 °C until RNA extraction.

In addition to the primary *hamp* analysis, a matched subset of UFE samples was further examined for a set of transcripts from selected iron- and antioxidant-related genes to determine whether UFE *hamp* transcript heterogeneity was accompanied by coordinated variation in these gene transcripts. The analyzed genes were *slc40a1* (solute carrier family 40 member 1; ferroportin), *tf* (transferrin), *tfr1*-like (transferrin receptor 1-like), and *sod3* (extracellular superoxide dismutase 3). The matched sample information, primer and assay details, source expression values, and correlation outputs for this analysis are provided in Supplementary Excel File S4.

2.2. RNA Extraction and cDNA Synthesis

Total RNA was extracted from unfertilized eggs and embryonic samples using TRIzol reagent (Thermo Fisher Scientific, Waltham, MA, USA), followed by on-column purification and DNase treatment with the RNeasy Mini Kit (Qiagen, Hilden, Germany), according to the manufacturers' instructions. RNA quantity and purity were assessed based on A260/A280 and A260/A230 ratios using a NanoDrop ND-1000 spectrophotometer (Thermo Fisher Scientific). Only RNA samples with A260/A280 and A260/A230 values of at least 1.9 and 2.0, respectively, were used for subsequent analyses. RNA integrity was checked using the RNA Integrity Number (RIN), with a minimum value of 7.0, on an Agilent 2100 Bioanalyzer (Agilent Technologies, Santa Clara, CA, USA).

First-strand cDNA was synthesized from 2 μg of total RNA using the Omniscript RT Kit (Qiagen) with a primer mixture of oligo$(dT)_{20}$ and random nonamers, according to the

manufacturer's instructions. After cDNA synthesis, each cDNA sample was checked by RT-qPCR using 3–4 laboratory-established common housekeeping genes, such as actins, GAPDHs, ribosomal proteins, and/or 18S rRNA, and Ct-log information was archived together with the cDNA records. Both original RT products and diluted cDNA templates were stored in aliquots at approximately −85 °C. When archived templates were reused, the same amplification conditions were applied, and Ct values were compared with archived technical replicate records to confirm consistency within the laboratory QC range. All cDNA samples were synthesized using the same RT kit described above, and the RT-qPCR analyses used the same reagent system described below. For a subset of archived samples, earlier cDNA preparations yielded RT-qPCR patterns consistent with those obtained in the final re-analysis of the full cDNA set.

2.3. Primer Design and Quantitative Real-Time PCR Analysis

The expression of *hamp* transcripts was quantified by real-time quantitative PCR (RT-qPCR) using primers designed from the Siberian sturgeon *hamp* sequence identified in our previous study [21]. Primer sequences, amplicon sizes, and amplification characteristics for *hamp* and the reference gene 18S rRNA are provided in Supplementary Table S2.

Because sturgeon genomes are characterized by lineage-specific genome duplication and paralog retention, the assay scope of the *hamp* qPCR primer set was further evaluated using the publicly available *Acipenser ruthenus* draft genome resource [fAciRut3.2 maternal haplotype (GCF_902713425.1)] together with our local NGS database for *A. baerii*. Sequence inspection showed that two annotated *hamp*-like loci are present in the draft genome of *A. ruthenus*, but their open reading frame (ORF) nucleotide sequences are identical, with only very small differences outside the coding region. Searches of our local *A. baerii* NGS resources from adult tissues, embryos, and larvae showed a similar pattern of highly conserved, closely related *hamp* transcript sequences. In these local *A. baerii* resources, single nucleotide polymorphism (SNP)-level differences were detected in the coding region, but they did not result in amino acid substitutions, indicating that the predicted peptide sequences encoded by these variants were identical. However, because the currently available *A. baerii* data do not allow us to determine whether the small sequence differences represent paralog-level or allele-level variation, we avoided copy-specific expression interpretation. Accordingly, the present assay was interpreted as measuring the combined abundance of closely related *hamp* transcripts amplified by the shared primer set, rather than strictly copy-specific expression. As an additional assay-robustness check, we tested whether different primer pairs designed to amplify different amplicon regions within the conserved ORF could generate comparable threshold cycle (Ct) ranges. Repeated tests using two additional *hamp* primer pairs consistently yielded Ct ranges highly similar to those observed with the original *hamp* primer pair (Supplementary Table S2). Primer pairs for the transcripts from selected iron- and antioxidant-related genes used in the UFE association analysis were either adopted from previous studies or newly designed for this study. Newly designed primers were developed using the same conserved-region targeting strategy described above for the *hamp* assay, based on publicly available *A. ruthenus* draft genome information and local *A. baerii* NGS resources where applicable. Relevant primer and assay information for these gene transcripts is provided in Supplementary Excel File S4.

For quantitative PCR (qPCR), the original RT product (cDNA) was diluted 10-fold with nuclease-free water and used as the template. Quantitative PCR was performed using LightCycler 480 SYBR Green I Master Mix (Roche Applied Science, Penzberg, Germany) on a LightCycler 480 Real-Time PCR System (Roche). Melt-curve analysis was performed after amplification to verify the presence of a single specific product. The Ct value of each biological replicate was determined as the mean Ct from triplicate amplifications,

corresponding to three technical replicates per cDNA template. Amplification efficiency was validated by the standard-curve method using four or five 10-fold serial dilutions of pooled cDNA samples (Supplementary Table S2).

2.4. Normalization of Expression Data and Statistical Analysis

Relative *hamp* transcript abundance was normalized to 18S rRNA, which had previously been validated as a stable reference gene for this developmental series [21,22]. Expression levels were calculated as normalized relative quantity (NRQ) values using the efficiency-corrected ΔCt method [23,24]. When required for statistical analysis, NRQ values were natural log-transformed and expressed as ln(NRQ). For unfertilized eggs, normalized *hamp* transcript abundance was analyzed across 17 different UFE batches to assess variation in maternal transcript loading and subsequently to examine potential correlations between UFE *hamp* transcript abundance and available metadata variables, including female traits such as age, body weight (BW), total length (TL), and condition factor (CF), sampling year, fertilization rate, and hatching rate. For embryonic samples from the five crosses (DevSeries 1–5), developmental expression patterns were analyzed by stage-wise NRQ comparisons among DevSeries and by NRQ comparisons across developmental stages within each DevSeries, in order to identify shared and DevSeries-associated patterns of *hamp* expression variation during embryogenesis (Table 1).

Table 1. Experimental datasets and analytical purposes used for the main analysis of *hamp* transcript abundance in Siberian sturgeon eggs and embryos.

Analysis Set	Analytical Unit	Dataset Coverage	Expression Variable	Analytical Purpose
UFE-17 maternal-loading dataset	Biological replicate pools from unfertilized egg batches	17 independent UFE batches collected between 2011 and 2025	UFE-stage NRQ and ln(NRQ)	To quantify among-batch variation in maternally loaded *hamp* transcript abundance
UFE-17 metadata matrix	Batch-level UFE means with available metadata	17 batch-level records with female-trait metadata; fertilization and hatching rates available for fertilized subsets	Batch-level mean ln(NRQ) and metadata variables	To examine exploratory associations with sampling year, repeated-female representation, female traits, reproductive output, and female-trait clustering
Developmental series dataset	Five selected developmental series linked to UFE batches	DevSeries 1–5, each spanning 13 developmental stages from UFE to FH	Stage-wise NRQ and ln(NRQ)	To describe developmental *hamp* expression profiles among selected DevSeries with distinct UFE baselines
UFE-normalized developmental matrix	Stage-wise values normalized to the corresponding UFE baseline of each DevSeries	Five DevSeries × 13 developmental stages	$\log_2$ fold change relative to the within-series UFE mean	To compare developmental changes relative to each series-specific maternal starting level
Formal temporal analysis set	ln(NRQ)-based DevSeries × stage matrix	Five DevSeries × 13 developmental stages with biological replicate structure	Estimated marginal means, model effects, interaction effects, and pairwise contrasts	To statistically evaluate developmental-stage effects, DevSeries effects, DevSeries × stage interaction, and stage-wise or within-series contrasts

UFE, unfertilized egg; FH, first hatch; NRQ, normalized relative quantity. Female-trait metadata included age, body weight, total length, and condition factor.

All statistical analyses were performed using IBM SPSS Statistics (version 29.0.2; IBM Corp., Armonk, NY, USA), and differences were considered statistically significant at $p < 0.05$. Differences in maternally loaded *hamp* transcript abundance among the 17 UFE batches were evaluated using Welch ANOVA followed by Games–Howell post hoc pairwise comparisons after assumption checks, including Shapiro–Wilk tests and Q–Q plot inspection for distributional/residual normality and Levene's homogeneity-of-variance tests. Effect-size estimates included η^2, ε^2, and ω^2 scores to quantitatively evaluate the magnitude of among-batch differences. Potential correlations of UFE *hamp* transcript abundance with female parameters, including age, BW, TL, and CF, as well as reproductive outcomes, including fertilization and hatching rates, were tested using Spearman's rank correlation tests with Benjamini–Hochberg false discovery rate (BH-FDR) adjustment. Year-related Spearman's correlation, regression-based checks including selected year-associated interaction terms, and repeated-female sensitivity assessments were conducted to evaluate whether the observed variability in UFE *hamp* transcript abundance could be explained primarily by sampling year or repeated use of the same female. Hierarchical clustering analyses using z-score-standardized female-trait variables with squared Euclidean distance and Ward linkage options were carried out to classify UFE batches according to combined female-trait profiles without using *hamp* expression values. Mann–Whitney U or Kruskal–Wallis tests were then performed according to the number of clusters to examine whether female clusters showed different distributions of maternally loaded *hamp* transcript abundance.

Differences in *hamp* expression levels across developmental stages and among DevSeries were assessed using two-way ANOVA within a general linear model (GLM) framework, including partial η^2 estimation for DevSeries, developmental stage, and the DevSeries × developmental stage interaction. As in the UFE analysis, normality, variance, and residual diagnostic assessments were performed using Shapiro–Wilk and Levene's tests, together with Q–Q plot inspection. Estimated marginal means (EMMs) with 95% confidence intervals were used for interpretation and visualization of developmental expression profiles. GLM simple-effect tests and Bonferroni-adjusted EMM pairwise comparisons were then used to quantify DevSeries-associated differences within each developmental stage and temporal expression variation across developmental stages within each DevSeries. For the UFE-stage association analysis of selected iron- and antioxidant-related gene transcripts described above, NRQ values were natural log-transformed before correlation analysis. Pairwise associations among the analyzed gene transcripts, including *hamp*, were evaluated using both Spearman's rank correlation and Pearson's correlation. Raw p values from the pairwise correlation tests were adjusted using the BH-FDR procedure. The statistical analysis workflow and rationale applied in this study are summarized in Supplementary Table S3.

3. Results

3.1. Differential Maternal Loading of Hamp Transcripts Among Independent Egg Batches

RT-qPCR analysis consistently detected *hamp* transcripts in all 17 unfertilized egg batches examined. For the UFE-17 dataset, maternal *hamp* transcript abundance was analyzed at the biological replicate-pool level and compared among independent UFE batches using ln-transformed NRQ values. Assumption diagnostics were first examined to define the appropriate statistical framework. Replicate-level ln(NRQ) values showed a strongly batch-structured distribution and deviated from normality by Shapiro–Wilk test ($W = 0.864$, $p < 0.001$), whereas residuals from the batch-comparison model showed no evidence of deviation from normality ($W = 0.985$, $p = 0.760$). Levene-type variance diagnostics were not fully consistent across centering methods ($p = 0.031$–0.932), and

Welch ANOVA was therefore used as the primary global test for among-batch comparison (Supplementary Figure S1; Supplementary Table S4), followed by Games–Howell post hoc comparisons.

Within this analytical framework, maternal *hamp* transcript abundance varied markedly among batches. In the sampling-order plot, replicate-pool values were displayed for each UFE batch together with the sampling year, allowing within-batch replicate dispersion and selected repeated-female comparisons to be inspected directly (Figure 1A). Among batches derived from the same female, Games–Howell post hoc comparisons did not detect a significant difference between UFE03 and UFE08 ($p > 0.05$), whereas UFE12 and UFE15 differed significantly ($p < 0.05$) (Figure 1A; Supplementary Figure S2). Significant among-batch differences were also observed among batches obtained in the same year or similar sampling period, including UFE05 versus UFE06 in 2016, UFE11 versus UFE12 in 2022, and the 2024 batches UFE14, UFE15, and UFE16 ($p < 0.05$) (Figure 1A; Supplementary Figure S2).

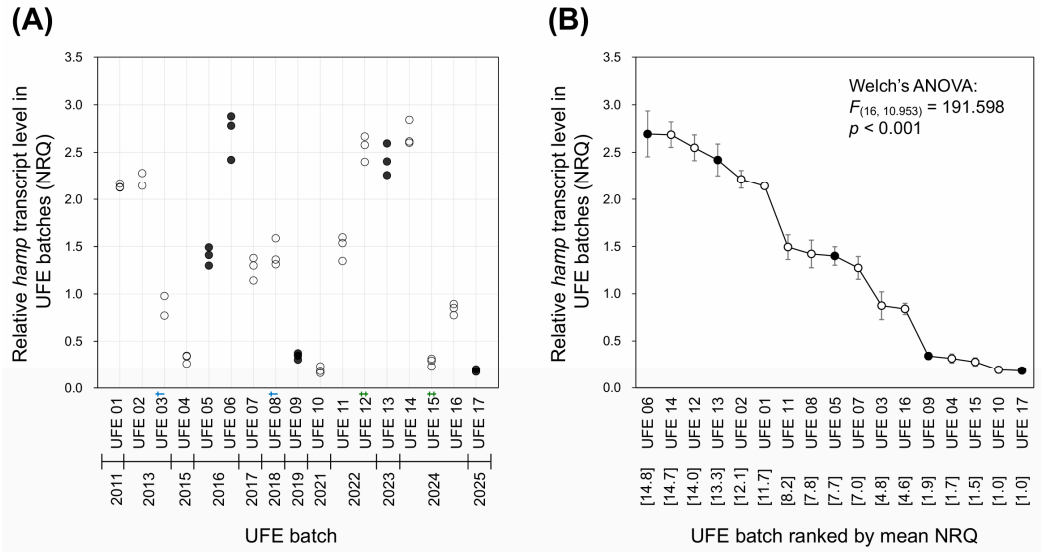

Figure 1. Batch-to-batch variation in maternal *hamp* transcript abundance among 17 unfertilized egg batches. (**A**) Relative *hamp* transcript abundance in individual biological replicate pools from 17 unfertilized egg (UFE) batches arranged by sampling year. Each point represents one biological replicate pool. Closed circles indicate UFE batches for which subsequent embryonic developmental profiling was performed, whereas open circles indicate batches analyzed only at the UFE stage. Symbols marked with the same dagger indicate UFE batches derived from the same female: †, UFE03 and UFE08; ‡, UFE12 and UFE15. (**B**) UFE batches ranked according to mean normalized relative quantity (NRQ). Points and error bars indicate mean ± SD. Bracketed values below batch labels indicate fold values relative to the lowest-ranked mean NRQ, showing an approximately 14.8-fold observed range across the 17 UFE batches. Welch ANOVA supported significant among-batch heterogeneity [F(16, 10.953) = 191.598, $p < 0.001$].

When batches were ranked according to their mean UFE NRQ values, maternal *hamp* transcript abundance spanned an approximately 14.8-fold observed range in NRQ values (0.182–2.693) across the 17 batches (Figure 1B). Welch ANOVA supported significant among-batch heterogeneity in UFE *hamp* transcript abundance [F(16, 10.953) = 191.598, $p < 0.001$], and the overall post hoc pairwise structure of this heterogeneity is summarized in Supplementary Figure S2.

Exploratory metadata-based analyses were further performed to examine potential associations with the observed UFE-level heterogeneity. In the interannual checks, sampling year was not significantly correlated with batch-level mean ln(NRQ) (Spearman's $\rho = -0.202$, $p = 0.437$). Regression models using z-score-standardized female parameters and sampling

year did not support a significant year-associated pattern, although the model including female condition factor and sampling year showed a borderline overall trend (R^2 = 0.336, adjusted R^2 = 0.241, p = 0.057) and a nominal positive coefficient for female condition factor (β = 0.517, p = 0.033); year terms and year-by-female-parameter interactions were not significant (Supplementary Table S5A). Reduced-dataset checks retaining only one record per repeated female also produced non-significant year-correlation results (ρ = −0.084 to −0.296, p = 0.284–0.765) (Supplementary Table S5B).

In Spearman correlation analyses, no female or reproductive parameter remained significant after BH-FDR correction, although female age showed a weak negative tendency and female condition factor showed a weak positive tendency; fertilization and hatching rates were not significantly associated with UFE *hamp* transcript abundance (Supplementary Table S5C). Female-trait clustering based on age, body weight, and condition factor also showed no significant cluster-wise differences in UFE *hamp* transcript abundance in the two-, three-, or four-cluster solutions (p = 0.245, 0.103, and 0.205, respectively) (Supplementary Figure S3; Supplementary Table S6).

3.2. Developmental Hamp Expression Profiles Relative to UFE Baselines in Five DevSeries

The five DevSeries exhibited distinguishable developmental expression profiles of *hamp* transcripts in relation to their initial UFE baselines. In the absolute NRQ heatmap, the five series showed a broad grouping tendency according to their temporal abundance patterns (Figure 2A). DevSeries 2 and DevSeries 4, which had relatively higher UFE baselines among the five selected series, maintained higher absolute *hamp* transcript abundance across much of the early developmental period. In contrast, DevSeries 3 and DevSeries 5, which had relatively lower UFE baselines, showed lower absolute abundance during most early stages. DevSeries 1 showed a mixed pattern, resembling the higher-baseline series during part of early development but becoming more similar to the lower-baseline series during later portions of the trajectory.

A comparable grouping tendency was also apparent when the same data were expressed as $\log_2$ fold change relative to the within-series UFE mean (Figure 2B). DevSeries 2 and DevSeries 4 showed broader periods of UFE-relative decrease or moderated change after the UFE stage, whereas DevSeries 3 and DevSeries 5 showed more evident UFE-relative increases at selected post-cleavage stages. DevSeries 1, despite its intermediate absolute NRQ profile, showed an overall UFE-relative decrease pattern without the positive UFE-relative elevations observed in DevSeries 3 and DevSeries 5. Source values for the NRQ and UFE-normalized $\log_2$FC matrices are provided in Supplementary Table S7, and the corresponding series-specific NRQ line plots are shown in Supplementary Figure S4.

To evaluate the DevSeries-specific developmental profiles statistically, the ln(NRQ)-based DevSeries × developmental-stage dataset was analyzed using a two-way GLM/ANOVA framework. The dataset was balanced, with five DevSeries, 13 developmental stages, and three biological replicate pools per DevSeries × stage cell. Model diagnostics showed no evidence of residual non-normality (Shapiro–Wilk W = 0.991, p = 0.256) or cell-wise variance heterogeneity across the full DevSeries × stage structure [Levene's F(64, 130) = 1.223, p = 0.167] (Supplementary Figure S5; Supplementary Table S8A,B).

The formal temporal model supported significant DevSeries, developmental-stage, and DevSeries × stage effects on *hamp* transcript abundance. The DevSeries × stage interaction was highly significant [F(48, 130) = 236.766, p < 0.001, partial η_p^2 = 0.989], indicating that developmental changes in ln(NRQ) differed among DevSeries rather than following a single shared temporal pattern (Figure 3A; Supplementary Table S8C). Stage-wise effect statistics showed that among-series differences were significant at all developmental stages, but their magnitude varied across embryogenesis. The between-series effect was large

during UFE-to-blastula stages and again around SYP, ON, SH, and TRH, whereas the effect size was comparatively reduced at ExcR, HR, and FH (Figure 3B). Full EMM values are provided in Supplementary Table S9.

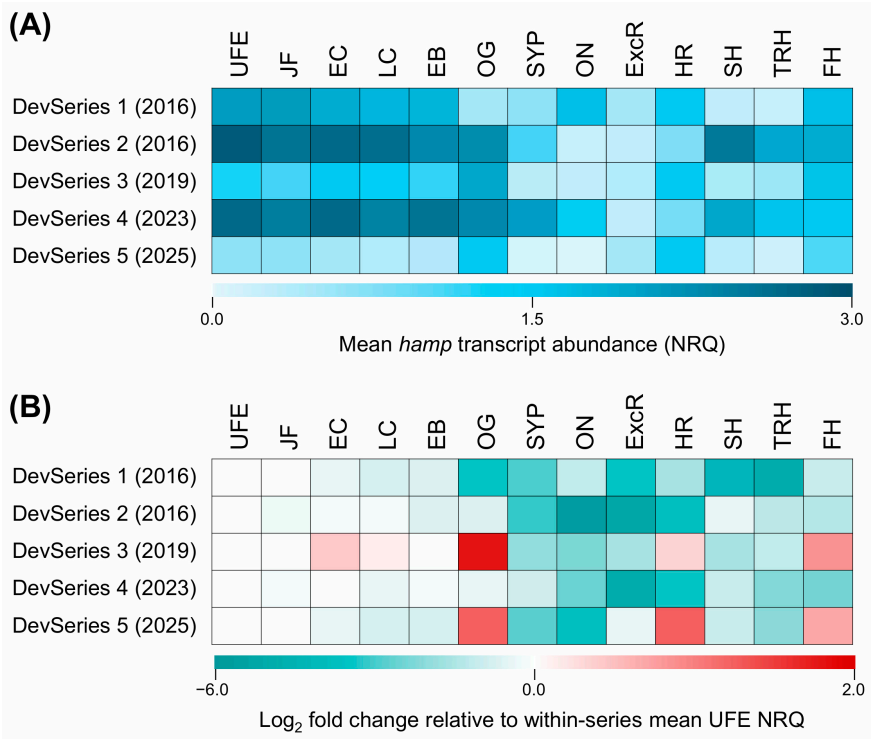

Figure 2. Heatmap overview of developmental *hamp* transcript abundance across five DevSeries. (**A**) Mean *hamp* transcript abundance, expressed as normalized relative quantity (NRQ), across 13 developmental stages from unfertilized eggs (UFE) to first hatch (FH). Each row represents one DevSeries, with the sampling year indicated in parentheses. Darker color intensity indicates higher mean NRQ values. (**B**) UFE-normalized developmental changes in *hamp* transcript abundance, expressed as $\log_2$ fold change relative to the within-series mean UFE NRQ. Negative values indicate lower abundance than the corresponding UFE baseline, whereas positive values indicate higher abundance relative to that baseline. UFE, unfertilized eggs; JF, just fertilized eggs; EC, early cleavage; LC, late cleavage; EB, early blastula; OG, onset of gastrulation; SYP, small yolk plug formed; ON, onset of neurulation; ExcR, excretory rudiments elongate; HR, heart rudiment; SH, S-shaped heart formed; TRH, tail end reaches head; FH, first hatch; NRQ, normalized relative quantity.

The stage-wise pairwise comparison heatmap further resolved how among-series differences varied across developmental stages (Supplementary Figure S6; Supplementary Excel File S2). During UFE-to-early embryonic stages, significant contrasts generally separated DevSeries 2 and DevSeries 4 from DevSeries 3 and DevSeries 5. This early contrast structure was not maintained uniformly across all stages. Around ExcR and HR, the pairwise contrast pattern was less pronounced than in the early stages, whereas distinct among-series contrasts were again observed around SH and TRH.

Within-series pairwise comparisons showed that each DevSeries had a distinct developmental-stage structure rather than a simple monotonic change (Supplementary Figure S7; Supplementary Excel File S3). DevSeries 2 and DevSeries 4 retained relatively high EMMs during early development, followed by marked decreases during post-gastrulation to early organogenesis stages and higher values again around SH. In the UFE-normalized matrix, however, both DevSeries 2 and DevSeries 4 remained below their own UFE baselines at FH. By contrast, DevSeries 3 and DevSeries 5 showed lower early-stage abundance but displayed local stage-associated increases, particularly around OG and/or HR, and their FH values exceeded the corresponding within-series UFE baselines.

DevSeries 1 showed an overall UFE-relative decrease after the earliest stages, with limited later-stage increases. These stage-wise and within-series patterns are summarized quantitatively in Table 2, including the UFE baseline position of each DevSeries and the post-UFE stages showing the highest and lowest UFE-normalized $\log_2$ fold-change values.

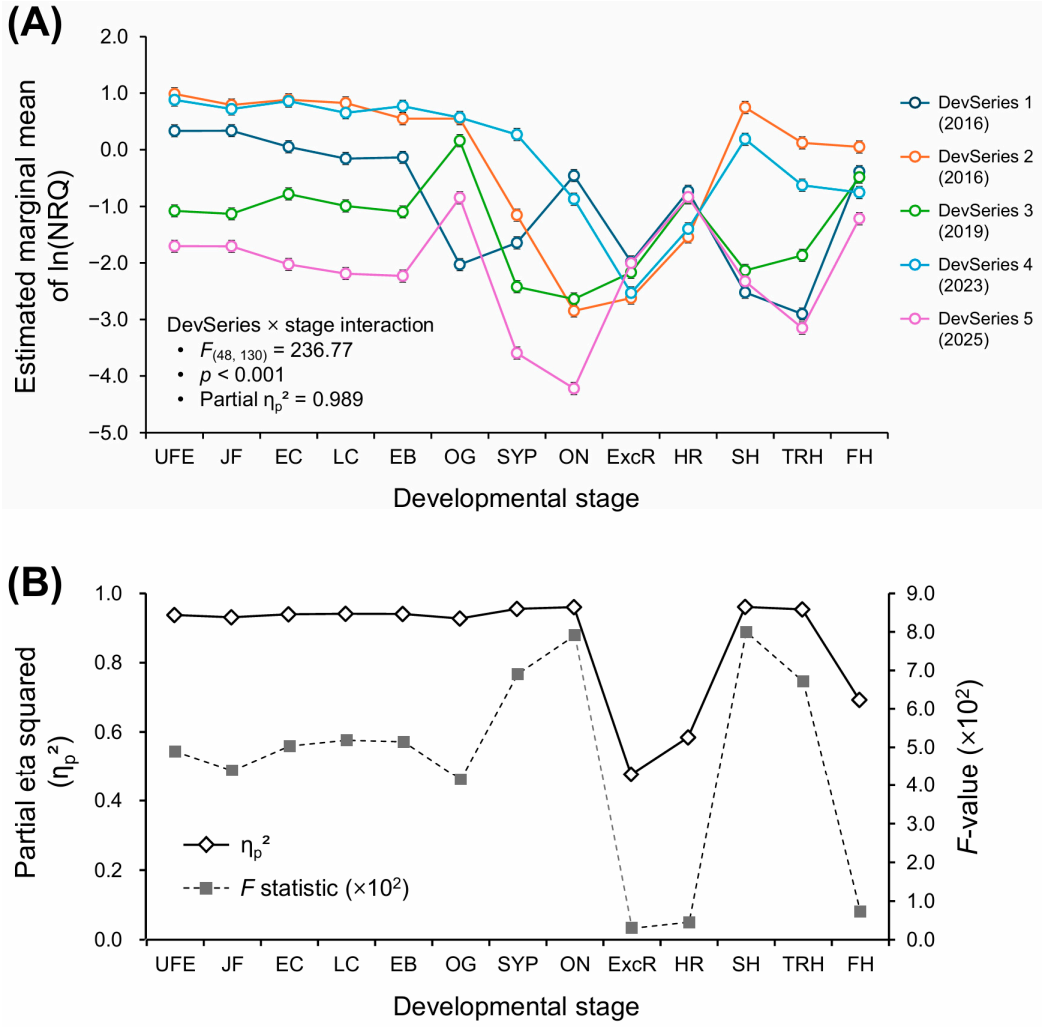

Figure 3. Formal temporal analysis of developmental *hamp* transcript expression profiles across five DevSeries. (**A**) Estimated marginal means (EMMs) of ln(NRQ) for *hamp* transcript abundance across 13 developmental stages in five DevSeries. EMMs were derived from the DevSeries × developmental-stage GLM using ln(NRQ) as the response variable. The DevSeries × stage interaction was significant [F(48, 130) = 236.77, $p < 0.001$, partial $\eta_p^2 = 0.989$], indicating DevSeries-specific developmental expression profiles. (**B**) Stage-wise among-DevSeries effect statistics. Partial eta squared (η_p^2) and F statistics are shown for the simple effect of DevSeries at each developmental stage; F statistics are scaled as $\times 10^2$. Stage abbreviations are defined in Figure 2 and in Section 2. NRQ, normalized relative quantity; EMM, estimated marginal mean.

Finally, an exploratory candidate-transcript analysis was performed in a matched subset of UFE samples to examine whether the observed *hamp* transcript heterogeneity was accompanied by coordinated variation in selected iron- and physiology-related transcripts. No tested association involving *hamp* transcript abundance remained significant after BH-FDR correction, indicating that the UFE-level *hamp* heterogeneity was not explained by a statistically supported co-expression pattern within this limited candidate set (Supplementary Excel File S4).

Table 2. Quantitative summary of five developmental series and their UFE-normalized expression patterns.

DevSeries (UFE Batch)	Female Age/BW/CF	Fertilization/ Hatching (%)	UFE ln(NRQ)	UFE Rank	Highest log_2FC (Post-UFE Stage)	Lowest log_2FC (Post-UFE Stage)	Δln(NRQ) FH–TRH
DS 1 (UFE 05)	13/12.2/0.638	89.5/80.1	0.334 ± 0.070	9/17	+0.001 (JF)	−4.672 (TRH)	+2.516 *
DS 2 (UFE 06)	13/18.1/0.635	95.1/77.0	0.988 ± 0.092	1/17	−0.154 (EC)	−5.537 (ON)	−0.072 ns
DS 3 (UFE 09)	16/7.1/0.450	90.5/69.4	−1.080 ± 0.106	13/17	+1.785 (OG)	−2.255 (ON)	+1.384 *
DS 4 (UFE 13)	20/11.9/0.528	90.5/69.1	0.882 ± 0.069	4/17	−0.032 (EC)	−4.926 (ExcR)	−0.129 ns
DS 5 (UFE 17)	22/29.2/0.600	91.5/72.1	−1.704 ± 0.080	17/17	+1.250 (HR)	−3.633 (ON)	+1.934 *

DS, DevSeries; BW, body weight (kg); TL, total length (cm); CF, condition factor = 100,000 × BW (kg)/TL $(cm)^3$; NRQ, normalized relative quantity. Developmental-stage abbreviations follow those defined in Section 2 and Figure 2. Each DevSeries represents one developmental expression dataset associated with a defined fertilized cross and spanning UFE to FH. UFE rank was determined from the batch-level mean ln(NRQ) among the 17 UFE batches, with rank 1 indicating the highest maternal *hamp* transcript abundance. Highest and lowest log_2FC values indicate the maximum and minimum UFE-normalized values among post-UFE stages within each DevSeries, with the corresponding stage shown in parentheses. Δln(NRQ) FH–TRH was calculated as FH mean ln(NRQ) minus TRH mean ln(NRQ). * Bonferroni-adjusted $p < 0.05$ for the within-series FH vs. TRH comparison; ns, not significant.

4. Discussion

4.1. UFE Hamp Transcript Heterogeneity as a Variable Maternal Baseline

The present study broadens the early developmental context of *hamp* transcript regulation in Siberian sturgeon. The consistent detection of *hamp* transcripts in unfertilized eggs indicates that this hepcidin-related transcript is included in the maternal RNA pool of this species. Given the basal phylogenetic position of sturgeons among actinopterygians, this finding extends the reproductive and early developmental context of *hamp* to a non-teleost lineage. Together with the established importance of iron regulation during oocyte maturation, including vitellogenin-mediated iron transport to growing oocytes, and subsequent embryogenesis [4,25–27], maternal *hamp* transcript loading in sturgeon eggs suggests that hepcidin-related maternal provisioning may represent an evolutionarily relevant component of the early developmental repertoire in externally fertilizing actinopterygians.

More importantly, the *hamp* transcript abundance levels vary markedly among independent spawning batches. In the expanded 17-batch UFE dataset, maternal *hamp* transcript abundance showed an approximately 14.8-fold observed range across 17 UFE batches, and the among-batch heterogeneity was robustly supported by formal statistical testing. These findings indicate that sturgeon embryos may begin development with substantially different *hamp* transcript baselines. In the present dataset, such apparent difference was observed even at the individual-female level, as the same female exhibited significantly different maternal loading levels in different spawning years. Furthermore, despite spawning within a short time frame, multiple female spawners that had been maintained under the same culture regime at the same facility for several years showed considerably different *hamp* transcript abundance levels. In this respect, maternal *hamp* transcript abundance should be regarded as a variable molecular starting state of individual spawning batches [11,13].

The expanded metadata-based analyses further indicate that the observed UFE heterogeneity cannot be reduced to a simple explanatory factor within the present dataset. Sampling year was not significantly associated with UFE *hamp* transcript abundance, and the available female traits did not remain significant after multiple-testing correction. Female age showed only a weak negative tendency, whereas female condition factor showed a weak positive tendency, but neither provided an FDR-supported explanation. Likewise, fertilization and hatching rates were not significantly associated with UFE *hamp* transcript abundance after correction. Female-trait clustering based on available broodstock parameters also failed to define groups with statistically distinct UFE *hamp* transcript levels. Therefore, the present data do not support interpreting UFE *hamp* abundance as a simple reflection of sampling year, female size or condition, or reproductive output.

Maternal transcript abundance in unfertilized eggs can be conceptually conflated with egg quality or developmental outcome in farmed fishes [25,28–30]. A previous transcriptomic study in Atlantic salmon proposed that the post-ovulatory *hamp* level could be considered as a potential egg quality marker based on repeated observations of high *hamp* accumulation only in poor quality eggs [14]. However, the present dataset did not support a direct association between the apparent heterogeneity in *hamp* abundance and fertilization or hatching performance.

We also explored whether UFE *hamp* transcript abundance was coordinated with several selected iron-related or antioxidant-related gene transcripts (*slc40a1*, *tf*, *tfr1*-like and *sod3*) [16,31,32] in a matched subset of UFE samples. However, no tested association involving *hamp* transcript abundance remained statistically supported after BH-FDR correction. However, because egg iron concentration and protein-level iron-handling activity were not measured, the meaning of present expression data is limited and inconclusive whether UFE *hamp* transcript abundance is related with the degree of iron burden in the egg.

Taken together, the present UFE-17 analyses indicate that maternal *hamp* transcript loading in Siberian sturgeon is a pronounced feature but the reason or mechanism responsible for significant abundance heterogeneity among batches is currently unexplained. The present study therefore positions UFE *hamp* abundance not as a direct marker of embryonic viability, but as a variable molecular baseline that should be considered when early developmental expression profiles are compared among independent crosses or spawning batches. Future studies with structured broodstock designs, direct egg biochemical measurements, broader transcriptomic screening, and post-hatch performance data will be needed to identify the maternal, environmental, physiological, or management-related factors that contribute to this variation [25,33].

4.2. Maternal Loading Level and Developmental Hamp Expression Profiles During Embryogenesis

Although the mechanisms underlying UFE *hamp* transcript heterogeneity remain unresolved, the five developmental series showed that differences in the initial maternal baseline were associated with distinct embryonic expression profiles. The heatmap analysis and the formal DevSeries × developmental-stage model both support this interpretation. The significant DevSeries × stage interaction indicates that developmental changes of *hamp* levels did not follow a single shared temporal pattern across all five DevSeries. Rather, the trajectorial patterns among DevSeries tended to be distinguishable depending on their starting UFE *hamp* levels.

The stage-wise and within-series comparisons further refined this non-uniform profiles. From the developmental stage-wise comparison, differences in *hamp* transcript levels among DevSeries were strong during UFE-to-early embryonic stages, became less pronounced around some organogenesis-related stages such as ExcR and HR, and were again evident around later stages including SH and TRH. On the other hand, within each DevSeries, the expression profile was not a simple monotonic decline or increase; rather, it displayed a 'complementary'-like change. In higher-baseline DevSeries (i.e., DevSeries 2 and DevSeries 4), the early maternal transcript pool remained comparatively high in absolute terms but did not produce FH values exceeding the UFE baseline. In lower-baseline DevSeries (DevSeries 3 and DevSeries 5), early absolute abundance was lower, but selected later stages, including FH, exceeded the corresponding UFE baseline.

These transcript-level patterns can be discussed in relation to major embryological transitions, although the mechanistic interpretation must remain cautious. The stage-associated increases or re-elevations observed around gastrulation, heart formation, and hatching-related stages coincide with developmental periods in which cell differentiation, morphogenetic movement, blood circulation-related maturation, and preparation for post-

hatch life become increasingly relevant. In vertebrate embryos, these processes are closely linked to iron handling, mitochondrial activity, oxidative balance, and hematopoietic or vascular development [5,16,34]. Previous model studies have also connected hepcidin and ferroportin regulation with embryonic iron homeostasis [4,16,35]. Within this broader context, the *hamp* transcript changes observed in Siberian sturgeon provide a biologically plausible developmental pattern, but they should not be interpreted as direct evidence that hepcidin-mediated iron regulation was functionally activated in the present embryos.

The late embryonic stages deserve particular attention because SH, TRH, and FH correspond to periods when circulation, body-axis completion, hatching readiness, and post-hatch behavioral transition become relevant in sturgeon development [19,20,25,36]. In externally developing fishes, the transition from chorion-protected embryo to hatched larva also increases direct exposure to the aquatic environment, where host-defense and nutritional-immunity pathways may become increasingly important [37–40]. In Siberian sturgeon, the first-hatch period is also associated with active behavioral transition, including upward swimming or negative geotaxis, which may impose new physiological demands on the newly hatched larvae [31,41]. These species-specific and stage-specific contexts make the FH-associated *hamp* transcript patterns biologically meaningful. However, this interpretation remains hypothetical at the transcript level and requires further validation.

Several limitations should be considered when interpreting these findings. First, the retrospective multi-year design remains a significant limitation because the UFE samples and developmental series were obtained between 2011 and 2025, and this design does not allow complete separation of variability associated with sampling year, breeding female, parental/cross background, and batch effects. Second, the observed associations between maternal *hamp* transcript load and embryonic expression profiles are correlational and cannot establish causal relationships. Third, the present study did not include complementary functional validation, such as protein-level analyses, immuno-histochemistry, direct iron measurements, or physiological assessments; therefore, the observed stage-associated changes should be interpreted primarily as descriptive transcript-level evidence of *hamp* expression variation, not as proof of hepcidin peptide activity, iron-regulatory function, immune function, or developmental-performance effects. In addition, unresolved paralog- or copy-specific expression and the inability to distinguish residual maternal transcripts from newly initiated zygotic transcription remain methodological limitations. Thus, although the present analyses provide statistical and metadata-based support for maternal *hamp* transcript heterogeneity and DevSeries-associated developmental expression profiles, their mechanistic and functional relevance should be evaluated in future studies specifically designed to address those questions.

5. Conclusions

The present findings indicate that developmental *hamp* expression in Siberian sturgeon should be interpreted in relation to the maternal transcript level present at the UFE stage. Maternal *hamp* transcript abundance differed markedly among UFE batches, and the subsequent developmental profiles differed among DevSeries when viewed relative to their own UFE starting levels. These results highlight the importance of considering spawning-batch-specific maternal transcript backgrounds when immune- and physiology-related genes are analyzed during early development in non-model fishes. In aquaculture research, this perspective may help refine the interpretation of spawning-batch variability, broodstock effects, and early embryo performance, while also providing a useful reference point for designing related studies in sturgeon fishes.

Supplementary Materials: The following supporting information can be downloaded at: https://www.mdpi.com/article/10.3390/fishes11070397/s1, Figure S1: Assumption diagnostics for among-batch analysis of maternally loaded *hamp* transcript abundance in 17 unfertilized egg batches. (A) Q–Q plot of ANOVA residuals for ln(NRQ) values. (B) Normality tests for residuals, showing no evidence of deviation from normality based on the Shapiro–Wilk test (W = 0.985, $p = 0.760$; $n = 49$). (C) Levene's tests for homogeneity of variances across the 17 UFE batches. The mean-based Levene test indicated variance heterogeneity ($p = 0.031$), whereas median-based tests were not significant, supporting the use of Welch ANOVA with Games–Howell post hoc comparisons for the primary among-batch analysis. NRQ, normalized relative quantity; UFE, unfertilized egg; Figure S2: Welch ANOVA and Games–Howell post hoc pairwise comparison matrix for UFE-stage *hamp* transcript abundance among 17 unfertilized egg batches. The heatmap shows Games–Howell post hoc *p*-value classes for pairwise comparisons of ln(NRQ) values among UFE batches following Welch ANOVA [$F(16, 10.953) = 191.598$, $p < 0.001$]. Gray cells indicate non-significant pairwise differences ($p \geq 0.05$), whereas increasing blue intensity indicates progressively stronger statistical significance ($p < 0.05$, $p < 0.01$, $p < 0.001$, and $p < 0.0001$); Figure S3: Female-trait clustering of UFE batches and cluster-wise comparison of maternally loaded *hamp* transcript abundance. (A) Hierarchical clustering of the 17 UFE batches based on z-score-standardized female traits, including age, body weight (BW), and condition factor (CF). The heatmap shows standardized values of each female-trait variable for the UFE batches grouped into three clusters (C1–C3). (B) Distribution of batch-level mean ln(NRQ) values of *hamp* transcripts among the three female-trait clusters. Cluster-wise differences in UFE *hamp* transcript abundance were not statistically significant based on the Kruskal–Wallis exact test ($H = 4.481$, df = 2, exact $p = 0.103$). Cluster means $\pm$ standard deviations were 0.523 ± 0.382 for C1, -0.559 ± 1.186 for C2, and -0.757 ± 1.122 for C3; Figure S4: Developmental profiles of relative *hamp* transcript abundance in five independent DevSeries. Relative *hamp* transcript levels are shown as normalized relative quantity (NRQ) values across developmental stages from UFE to FH in (A) DevSeries 1, (B) DevSeries 2, (C) DevSeries 3, (D) DevSeries 4, and (E) DevSeries 5. Points and error bars indicate mean $\pm$ SD of three biological replicate pools at each developmental stage; Figure S5: Diagnostic assessment of the ln(NRQ)-based DevSeries $\times$ developmental-stage GLM/ANOVA model for embryonic *hamp* expression analysis. (A) Q–Q plot of standardized residuals. (B) Frequency distribution of standardized residuals. (C) Scatter plot of standardized residuals against fitted ln(NRQ) values. (D) Summary of diagnostic results for the balanced developmental dataset, consisting of five DevSeries, 13 developmental stages, and three biological replicate pools per DevSeries $\times$ stage cell. Residual normality was supported by the Shapiro–Wilk test (W = 0.991, $p = 0.256$), and cell-wise homogeneity of variance was supported by Levene's test [$F(64, 130) = 1.223$, $p = 0.167$]; Figure S6: Stage-wise pairwise comparisons of *hamp* transcript abundance among DevSeries based on GLM-estimated marginal means. The heatmap summarizes Bonferroni-adjusted pairwise comparisons of ln(NRQ)-based estimated marginal means among DevSeries within each developmental stage. Each column represents a DevSeries pair, and ΔEMM was calculated as the estimated marginal mean of the first-listed series minus that of the second-listed series. Color direction indicates whether the first-listed DevSeries showed a lower or higher EMM than the second-listed DevSeries, and color intensity indicates the Bonferroni-adjusted *p*-value class. Gray cells indicate no significant difference. EMM, estimated marginal mean; Figure S7: Within-series developmental-stage pairwise comparisons of *hamp* transcript abundance based on GLM-estimated marginal means. Lower-triangle heatmaps summarize Bonferroni-adjusted pairwise comparisons of ln(NRQ)-based estimated marginal means among developmental stages within (A) DevSeries 1, (B) DevSeries 2, (C) DevSeries 3, (D) DevSeries 4, and (E) DevSeries 5. ΔEMM was calculated as the estimated marginal mean of the row-listed stage minus that of the column-listed stage. Color direction indicates whether the row-listed stage showed a lower or higher EMM than the column-listed stage, and color intensity indicates the Bonferroni-adjusted *p*-value class. Gray cells indicate no significant difference. EMM, estimated marginal mean; Table S1: Metadata for the 17 unfertilized egg batches analyzed for maternal *hamp* transcript abundance; Table S2: Sample structure, biological replicate definition, and qPCR assay information used in this study; Table S3: Statistical analysis workflow and rationale applied in this study; Table S4:

Assumption checks and primary statistical tests for among-batch comparison of UFE *hamp* transcript abundance; Table S5: Interannual effect, repeated-female checks, and female/reproductive-parameter correlations in the 17-batch UFE dataset; Table S6: Female-trait clustering statistics and cluster-wise comparison of UFE *hamp* abundance; Table S7: DevSeries source values for NRQ, ln(NRQ), and UFE-normalized $\log_2$ FC; Table S8: DevSeries model diagnostics and GLM/two-way ANOVA results; Table S9: Estimated marginal means for DevSeries × stage; File S1: Full Games–Howell post hoc comparisons among the 17 unfertilized egg (UFE) batches; File S2: Full stage-wise pairwise comparisons among developmental series (DevSeries); File S3: Full within-series developmental-stage pairwise comparisons; File S4: Matched-subset exploratory qPCR screening and co-expression analysis of hepcidin/iron-related candidate transcripts in unfertilized eggs.

Author Contributions: Conceptualization, Y.K.N.; Data curation, Y.K.N. and E.J.K.; Formal analysis, Y.K.N.; Funding acquisition, Y.K.N.; Methodology, E.J.K.; Resources, Y.K.N. and E.J.K.; Supervision, Y.K.N.; Writing—original draft, Y.K.N. All authors have read and agreed to the published version of the manuscript.

Funding: This work was supported by the National Research Foundation of Korea (NRF) grant funded by the Korea government (Ministry of Science and ICT; No. RS-2024-00405986).

Institutional Review Board Statement: Sampling of fish embryos, followed by dry-ice preservation and transport to the research institution, was not subject to mandatory animal ethics approval numbering under the institutional guidelines. Where applicable, subsequent experiments using some of these materials were conducted under separately approved protocols of Pukyong National University (approval nos. 2018-16, 2018-18, and 2024-75; approval date: 30 August 2018, 30 August 2018, 12 December 2024).

Informed Consent Statement: Not applicable.

Data Availability Statement: All relevant data are included within the article and its Supplementary Materials. Additional raw data supporting the findings of this study are available from the corresponding author upon reasonable request.

Acknowledgments: The authors would like to express their sincere gratitude to Chulhong Park of Dinoville Sturgeon Farm (Hamyang, South Korea) for his generous support in providing the Siberian sturgeon breeding materials used in this study.

Conflicts of Interest: The authors declare no conflicts of interest.

Abbreviations

The following abbreviations are used in this manuscript:

NRQ	Normalized relative quantity
RT-qPCR	Real-time quantitative polymerase chain reaction
UFE	Unfertilized egg
JF	Just fertilized egg
EC	Early cleavage
LC	Late cleavage
EB	Early blastula
OG	Onset of gastrulation
SYP	Small yolk plug formed
ON	Onset of neurulation
ExcR	Excretory rudiments elongate
HR	Heart rudiment
SH	S-shaped heart formed
TRH	Tail end reaches head
FH	First hatch

References

1. Shi, J.; Camus, A.C. Hepcidins in amphibians and fishes: Antimicrobial peptides or iron-regulatory hormones? *Dev. Comp. Immunol.* **2006**, *30*, 746–755. [CrossRef] [PubMed]
2. Masso-Silva, J.A.; Diamond, G. Antimicrobial peptides from fish. *Pharmaceuticals* **2014**, *7*, 265–310. [CrossRef] [PubMed]
3. Zhao, L.; Xia, Z.; Wang, F. Zebrafish in the sea of mineral (iron, zinc, and copper) metabolism. *Front. Pharmacol.* **2014**, *5*, 33. [CrossRef] [PubMed]
4. Sangkhae, V.; Fisher, A.L.; Chua, K.J.; Ruchala, P.; Ganz, T.; Nemeth, E. Maternal hepcidin determines embryo iron homeostasis in mice. *Blood* **2020**, *136*, 2206–2216. [CrossRef] [PubMed]
5. Donker, A.E.; van der Staaij, H.; Swinkels, D.W. The critical roles of iron during the journey from fetus to adolescent: Developmental aspects of iron homeostasis. *Blood Rev.* **2021**, *50*, 100866. [CrossRef] [PubMed]
6. Liu, M.; Peng, M.; Ma, J.; Hu, R.; Xu, Q.; Hu, P.; Chen, L. Hepcidin deficiency disrupts iron homeostasis and induces ferroptosis in zebrafish liver. *Fishes* **2025**, *10*, 243. [CrossRef]
7. Rauwerda, H.; Wackers, P.; Pagano, J.F.B.; de Jong, M.; Ensink, W.; Dekker, R.; Nehrdich, U.; Spain, H.P.; Jonker, M.; Breit, T.M. Mother-specific signature in the maternal transcriptome composition of mature, unfertilized zebrafish eggs. *PLoS ONE* **2016**, *11*, e0147151. [CrossRef] [PubMed]
8. Ahi, E.P.; Singh, P.; Lecaudey, L.A.; Gessl, W.; Sturmbauer, C. Maternal mRNA input of growth and stress-response-related genes in cichlids in relation to egg size and trophic specialization. *EvoDevo* **2018**, *9*, 23. [CrossRef] [PubMed]
9. Vastenhouw, N.L.; Cao, W.X.; Lipshitz, H.D. The maternal-to-zygotic transition revisited. *Development* **2019**, *146*, dev161471. [CrossRef]
10. Niepagen, N.; Bertolini, F.; Berg, L.; Tomkiewicz, J.; Kjørsvik, E. Maternal provisioning and zygotic activation: Transcriptomic dynamics of early Atlantic halibut (*Hippoglossus hippoglossus*) embryogenesis. *Front. Cell Dev. Biol.* **2025**, *13*, 1723170. [CrossRef] [PubMed]
11. Seppola, M.; Johnsen, H.; Mennen, S.; Myrnes, B.; Tveiten, H. Maternal transfer and transcriptional onset of immune genes during ontogenesis in Atlantic cod. *Dev. Comp. Immunol.* **2009**, *33*, 1205–1211. [CrossRef] [PubMed]
12. Gibert, Y.; Lattanzi, V.J.; Zhen, A.W.; Vedder, L.; Brunet, F.; Faasse, S.A.; Babitt, J.L.; Lin, H.Y.; Hammerschmidt, M.; Fraenkel, P.G. BMP signaling modulates hepcidin expression in zebrafish embryos independent of hemojuvelin. *PLoS ONE* **2011**, *6*, e14553. [CrossRef] [PubMed]
13. Wang, Y.; Liu, X.; Ma, L.; Yu, Y.; Yu, H.; Mohammed, S.; Chu, G.; Mu, L.; Zhang, Q. Identification and characterization of a hepcidin from half-smooth tongue sole *Cynoglossus semilaevis*. *Fish. Shellfish Immunol.* **2012**, *33*, 213–219. [CrossRef] [PubMed]
14. Bizuayehu, T.T.; Mommens, M.; Sundaram, A.Y.M.; Dhanasiri, A.K.S.; Babiak, I. Postovulatory maternal transcriptome in Atlantic salmon and its relation to developmental potential of embryos. *BMC Genom.* **2019**, *20*, 315. [CrossRef] [PubMed]
15. Ugolini, M.; Vastenhouw, N.L. Maternally loaded RNAs: No time to die. *Cell Res.* **2022**, *32*, 707–708. [CrossRef] [PubMed]
16. Yang, W.; Peng, M.; Wang, Y.; Zhang, X.; Li, W.; Zhai, X.; Wu, Z.; Hu, P.; Chen, L. Deletion of hepcidin disrupts iron homeostasis and hematopoiesis in zebrafish embryogenesis. *Development* **2025**, *152*, dev204307. [CrossRef] [PubMed]
17. Du, K.; Stöck, M.; Kneitz, S.; Klopp, C.; Woltering, J.M.; Adolfi, M.C.; Feron, R.; Prokopov, D.; Makunin, A.; Kichigin, I.; et al. The sterlet sturgeon genome sequence and the mechanisms of segmental rediploidization. *Nat. Ecol. Evol.* **2020**, *4*, 841–852. [CrossRef] [PubMed]
18. Höhne, C.; Prokopov, D.; Kuhl, H.; Du, K.; Klopp, C.; Wuertz, S.; Trifonov, V.; Stöck, M. The immune system of sturgeons and paddlefish (Acipenseriformes): A review with new data from a chromosome-scale sturgeon genome. *Rev. Aquac.* **2021**, *13*, 1709–1729. [CrossRef]
19. Kim, E.J.; Kim, K.H.; Nam, Y.K. Molecular characterization of hemopexin in the Siberian sturgeon (*Acipenser baerii*): Evolutionary insights and differential expression under immune and thermal stresses. *Int. J. Mol. Sci.* **2025**, *26*, 7934. [CrossRef] [PubMed]
20. Park, C.; Lee, S.Y.; Kim, D.S.; Nam, Y.K. Embryonic development of Siberian Sturgeon *Acipenser baerii* under hatchery conditions: An image guide with embryological descriptions. *Fish. Aquat. Sci.* **2013**, *16*, 15–23. [CrossRef]
21. Kim, C.H.; Kim, E.J.; Nam, Y.K. Chondrostean sturgeon hepcidin: An evolutionary link between teleost and tetrapod hepcidins. *Fish. Shellfish. Immunol.* **2019**, *88*, 117–125. [CrossRef] [PubMed]
22. Kim, C.H.; Kim, E.J.; Nam, Y.K. Subfunctionalization and evolution of liver-expressed antimicrobial peptide 2 (LEAP2) isoform genes in Siberian sturgeon (*Acipenser baerii*), a primitive chondrostean fish species. *Fish. Shellfish Immunol.* **2019**, *93*, 161–173. [CrossRef] [PubMed]
23. Livak, K.J.; Schmittgen, T.D. Analysis of relative gene expression data using real-time quantitative PCR and the $2^{-\Delta\Delta CT}$ method. *Methods* **2001**, *25*, 402–408. [CrossRef] [PubMed]
24. Schmittgen, T.D.; Livak, K.J. Analyzing real-time PCR data by the comparative CT method. *Nat. Protoc.* **2008**, *3*, 1101–1108. [CrossRef] [PubMed]
25. Kim, C.H.; Kim, E.J.; Seo, C.H.; Nam, Y.K. Transcriptome analysis of maternal gene transcripts in unfertilized eggs of *Misgurnus anguillicaudatus* and identification of immune-related maternal genes. *Int. J. Mol. Sci.* **2020**, *21*, 3872. [CrossRef] [PubMed]

26. Reading, B.J.; Andersen, L.K.; Ryu, Y.W.; Mushirobira, Y.; Todo, T.; Hiramatsu, N. Oogenesis and egg quality in finfish: Yolk formation and other factors influencing female fertility. *Fishes* **2018**, *3*, 45. [CrossRef]
27. Hara, A.; Hiramatsu, N.; Fujita, T. Vitellogenesis and choriogenesis in fishes. *Fish. Sci.* **2016**, *82*, 187–202. [CrossRef]
28. Sullivan, C.V.; Chapman, R.W.; Reading, B.J.; Anderson, P.E. Transcriptomics of mRNA and egg quality in farmed fish: Some recent developments and future directions. *Gen. Comp. Endocrinol.* **2015**, *221*, 23–30. [CrossRef] [PubMed]
29. Weber, G.M.; Birkett, J.; Martin, K.; Dixon, D.; Gao, G.; Leeds, T.D.; Vallejo, R.L.; Ma, H. Comparisons among rainbow trout, *Oncorhynchus mykiss*, populations of maternal transcript profile associated with egg viability. *BMC Genom.* **2021**, *22*, 448. [CrossRef] [PubMed]
30. Żarski, D.; Le Cam, A.; Frohlich, T.; Kösters, M.; Klopp, C.; Nynca, J.; Ciesielski, S.; Sarosiek, B.; Dryl, K.; Montfort, J.; et al. Neurodevelopment vs. the immune system: Complementary contributions of maternally-inherited gene transcripts and proteins to successful embryonic development in fish. *Genomics* **2021**, *113*, 3811–3826. [CrossRef] [PubMed]
31. Kim, C.H.; Kim, E.J.; Nam, Y.K. Superoxide dismutase multigene family from a primitive chondrostean sturgeon, *Acipenser baerii*: Molecular characterization, evolution, and antioxidant defense during development and pathogen infection. *Antioxidants* **2021**, *10*, 232. [CrossRef] [PubMed]
32. Kim, E.J.; Nam, Y.K. Expression characteristics of transferrin gene during embryo development and prolarval ontogeny in Siberian sturgeon *Acipenser baerii*. *Kor. J. Fish. Aquat. Sci.* **2024**, *57*, 41–52.
33. Guerrero-Tortolero, D.A.; Campos-Ramos, R. Maternal transcriptome biomarkers for egg quality in longfin yellowtail *Seriola rivoliana*. *Aquaculture* **2026**, *613*, 743442. [CrossRef]
34. Lv, P.; Gao, S.; Liu, F. Heme-deficient primitive red blood cells induce HSPC ferroptosis by altering iron homeostasis during zebrafish embryogenesis. *Development* **2023**, *150*, dev201690. [CrossRef] [PubMed]
35. Fraenkel, P.G.; Gibert, Y.; Holzheimer, J.L.; Lattanzi, V.J.; Burnett, S.F.; Dooley, K.A.; Wingert, R.A.; Zon, L.I. Transferrin-a modulates hepcidin expression in zebrafish embryos. *Blood* **2009**, *113*, 2843–2850. [CrossRef] [PubMed]
36. Shah, M.A.; Xie, X.; Rodina, M.; Stundl, J.; Braasch, I.; Šindelka, R.; Rzepkowska, M.; Saito, T.; Pšenička, M. Sturgeon gut development: A unique yolk utilization strategy among vertebrates. *Front. Cell Dev. Biol.* **2024**, *12*, 1358702. [CrossRef]
37. Olafsen, J.A. Interactions between fish larvae and bacteria in marine aquaculture. *Aquaculture* **2001**, *200*, 223–247. [CrossRef]
38. De la Paz, J.F.; Anguita-Salinas, C.; Díaz-Celis, C.; Chávez, F.P.; Allende, M.L. The zebrafish perivitelline fluid provides maternally-inherited defensive immunity. *Biomolecules* **2020**, *10*, 1274. [CrossRef] [PubMed]
39. Valero, Y.; Saraiva-Fraga, M.; Costas, B.; Guardiola, F.A. Antimicrobial peptides from fish: Beyond the fight against pathogens. *Rev. Aquac.* **2020**, *12*, 224–253. [CrossRef]
40. Murdoch, C.C.; Skaar, E.P. Nutritional immunity: The battle for nutrient metals at the host–pathogen interface. *Nat. Rev. Microbiol.* **2022**, *20*, 657–670. [CrossRef]
41. Kim, E.J.; Park, C.; Nam, Y.K. Behavioral characteristics of a chondrostean sturgeon species *Acipenser baerii* prelarvae in response to different environmental light intensities in a diel photoperiodic cycle. *J. Anim. Reprod. Biotechnol.* **2020**, *35*, 245–257. [CrossRef]